Effect of Fluorine on Near-Liquidus Phase Equilibria of an Fe-Mg Rich Basalt

Justin Filiberto[1, 2, 3], Justin Wood[2,4], Rajdeep Dasgupta [3], Nobumichi Shimizu[6], Loan Le[5], and Allan H. Treiman[2]

[1]Southern Illinois University - Carbondale, Department of Geology, 1259 Lincoln Dr, Carbondale, Il 62901

[2]Lunar and Planetary Institute, USRA, 3600 Bay Area Blvd, Houston, TX 77058

[3]Rice University, Department of Earth Science, 6100 Main St Houston TX 77005

[4]Rutgers University, Newark College of Arts and Sciences, Newark, NJ 07102

[5]Jacobs Sverdrup, Engineering Science Contract Group, Houston, Texas 77058

[6] Woods Hole Oceanographic Institution, Woods Hole, MA

Abstract

Volatile species (H_2O, CO_2, F, Cl, etc) have important effects on the formation and crystallization history of basaltic magmas. Here, we have experimentally investigated the effects of F on phase equilibria of Fe-Mg-rich basalt. Our results show that fluorine has large effects on the liquidus temperature and the chemistry of crystallizing minerals. Compared to the F-free system, addition of ~2 wt.% F moves the olivine-pigeonite liquidus point down ~2 kbar and 95 °C (from 12 kbar, 1375 °C to 10 kbar, 1280 °C). With increasing fluorine concentrations, $Kd^{Fe-Mg}_{Mineral-Melt}$ dramatically increases for both pyroxene and olivine, suggesting that fluorine in basaltic magmas complexes primarily with MgO. Complexing with MgO in the melt decreases its MgO activity, and forces the

crystallizing minerals to greater Fe/Mg, and so increases $Kd^{Fe-Mg}_{Mineral-Melt}$. Models of basalt generation, where the magma is fluorine-rich, need to include the effect of not only water but fluorine on liquidus depression and minerals crystallizing/melting. Our results suggest that fluorine may significantly aid in the petrogenesis of silica-poor, alkali-rich magmas in the Earth and Mars.

Keywords: halogens, martian meteorites, alkali basalts, basalt crystallization, phase equilibria, fluorine

1. **Introduction**

Volatile species (H_2O, CO_2, F, Cl, etc) are important in basalt genesis and mantle melting in arc, plume, ridge, and other planetary tectono-magmatic settings. Previous experimental work has mainly focused on the effects of water and carbon dioxide on liquidus temperature, phase relations, and compositions of basalts produced in these systems (e.g., Danyushevsky, 2001; Dasgupta et al., 2007; Feig et al., 2010; Feig et al., 2006; Gaetani and Grove, 1998; Gerbode and Dasgupta, 2010; Green, 1970; Grove et al., 2002; Grove et al., 2006; Médard and Grove, 2008; Mysen, 1975; Nekvasil et al., 2004). The effects of halogens in general, and those of fluorine in particular, have received far less attention (e.g., Brey et al., 2009; Filiberto and Treiman, 2009a; Filiberto and Treiman, 2009b; Foley et al., 1986). However, melts in planetary interiors can have non-negligible halogen concentrations, and the importance of chlorine and fluorine in basalt petrogenesis has been emphasized in recent literature both for Earth (Aoki et al., 1981; Brey et al., 2009) and Mars (Filiberto and Treiman, 2009a,b). Here, we explore the effects of fluorine on near-liquidus phase equilibria of a basalt.

Fluorine concentrations in terrestrial magmas: Evolved magmas (rhyolites and phonolites) can contain more than 5 wt% F (e.g., Carroll and Webster, 1994; Giordano et al., 2004; Harms and Schmincke, 2000; Webster et al., 1997); basaltic magmas typically contain less F than their evolved counter parts as summarized by Aoki et al. (1981) and Stecher (1998) for continental and oceanic basaltic rocks. They found that the abundance of F typically correlates with that of K_2O for most basaltic magmas, although this correlation breaks down at high K_2O concentrations. In tholeiites, F concentrations range from 30 to 1000 ppm (Aoki et al., 1981; Stecher, 1998; Yoshida et al., 1971); higher

primitive fluorine concentrations are seen in alkali rich rocks: nephelinites and kimberlites have concentrations up to 2000 ppm; and some lamproites contain up to 20,000 ppm (2 wt%) F (Aoki et al., 1981). This suggests that fluorine may be especially important for alkali-rich basaltic magmas. For example, primitive mantle of the Earth is estimated to have 25 ppm F (McDonough and Sun, 1995), thus with bulk partition coefficient of ~0.08 during mantle melting (Dalou et al., 2012), 0.1 to 2 wt.% partial melts will have F concentration of ~300 ppm (**Figure 1**).

Fluorine concentrations in martian magmas: Less is known about the fluorine concentrations of martian magmas. Bulk fluorine contents of the martian basalts (meteorites) are similar to those of terrestrial tholeiites (29-41 ppm, Dreibus and Wänke, 1985). But based on the F to Ti ratio, martian basalts and the bulk martian mantle are thought to be 2-3 times richer in F (and other halogens) than terrestrial basalts and mantle (Dreibus and Wänke, 1987; Treiman et al., 1986). If the F content of the martian mantle were three times greater than that of the Earth, similar low degree partial melting (as in the example above, 0.1-2 wt. %) should yield magmas with 950 to 750 ppm F (**Figure 1**). Further, alkalic basalts (typically rich in fluorine on Earth) have been suggested to occur, and maybe significant, on Mars (Dunn et al., 2007; McSween et al., 2006; Nekvasil et al., 2007). All of this, and the chemistry of volatile-bearing minerals in martian meteorites (amphiboles and apatite) suggests that fluorine, like chlorine (Filiberto and Treiman, 2009a; Filiberto and Treiman, 2009b; Patiño Douce and Roden, 2006; Patiño Douce et al., 2011), may be an important factor controlling basalt genesis in Mars (possibly to the extent of replacing water as the dominant volatile species).

Previous work on fluorine in igneous systems: Previous studies on fluorine in magmatic systems have mainly focused on the solubility mechanisms of F in aluminosilicate (+/-Na) melt and its effect on melt viscosity (Liu and Nekvasil, 2002; Liu and Tossell, 2003; Mysen et al., 2004; Schaller et al., 1992; Zeng et al., 1999). Nuclear magnetic resonance (NMR) studies of aluminosilicate glasses have shown that fluorine preferentially complexes with Al and possibly Si (Liu and Nekvasil, 2002; Liu and Tossell, 2003; Schaller et al., 1992; Zeng et al., 1999). For Na-aluminosilicate glasses four predominant complexes have been identified: Na-F, Na-Al-F (with Al in 4-fold coordination), Na-Al-F (with Al in 6-fold coordination), and Al-F (with Al in 6-fold coordination) (Mysen et al., 2004; Zeng and Stebbins, 2000). By complexing predominantly with Al in silica-rich magmas, F decreases their viscosity by depolymerizing the melt (Dingwell, 1989; Dingwell and Hess, 1998; Dingwell et al., 1985; Giordano et al., 2004; Zimova and Webb, 2007). This is a similar effect on melt structure and viscosity as dissolved water (e.g., Giordano et al., 2004).

Similar to NMR studies, most experiments on phase equilibria in F-bearing magmas have been on granitic or simplified systems (e.g, Dolejs and Baker, 2007a; Dolejs and Baker, 2007b; Foley et al., 1986; Lukkari and Holtz, 2007; Manning, 1981; Scaillet and MacDonald, 2001; Scaillet and MacDonald, 2003; Scaillet and Macdonald, 2006; Weidner and Martin, 1987; Xiao-lin et al., 1999; Xiong et al., 2002). Fluorine has dramatic effects on crystallizing phases (e.g, Dolejs and Baker, 2007a; Dolejs and Baker, 2007b; Foley et al., 1986; Manning, 1981). At 1 bar, in the Qz-Ab-Or-H_2O system, addition of fluorine shifts the boundary of the quartz-alkali feldspar liquidus field away from the quartz apex; addition of 4 %wt F shifts the minimum melting compositions from

100 $Qz_{37}Ab_{34}Or_{29}$ to $Qz_{15}Ab_{58}Or_{27}$ (Manning, 1981). In the $NaAlSiO_4$-$CaMgSi_2O_6$-SiO_2
101 system, also at 1 bar, fluorine reduces the liquidus temperature and changes the
102 compositions of the liquids produced (Luth, 1988a). For example, the liquid in
103 equilibrium with diopside at 1250° C in the F-bearing experiments is $Di_{56}Ab_{44}$ compared
104 with $Di_{33}Ab_{67}$ in the F-free experiments. The results suggests that F is complexing with
105 Ca and Mg in the liquid in a $NaAlSiO_4$-$CaMgSi_2O_6$-SiO_2 simplified system (Luth,
106 1988a). At higher pressure (28 kbar) in the $KAlSiO_4$-Mg_2SiO_4-SiO_2 system, fluorine
107 expands the field of enstatite stability with respect to that of forsterite by complexing
108 with Mg, K, and Al in the melt (Foley et al., 1986).

109 However, the solution mechanism for F in natural basaltic melts maybe more
110 complicated than in the simple systems. Recent NMR work has shown that a significant
111 proportion (>30%) of dissolved fluorine complexes with Mg (Kiczenski et al., 2004);
112 while experimental results combined with NMR and Raman spectroscopy studies have
113 suggested that F may complex with Ca (Luth, 1988b; Zeng and Stebbins, 2000). Fluorine
114 complexation with cations other than Al will not only lower the liquidus and affect the
115 viscosity, but also change the phase relations of crystallizing magmas. However, these
116 complexations are presumably bulk composition dependent.

117 In order to understand how fluorine behaves in a Si-poor, Mg, Fe-rich basaltic
118 system we have experimentally determined near liquidus phase relations of a synthetic
119 basalt doped with F. The results of these experiments can be directly compared with our
120 previous work on the same synthetic basalt conducted nominally volatile-free (Filiberto
121 et al., 2008) and doped with chlorine (Filiberto and Treiman, 2009a).

122 **2. Methods**

123 *2.2 Experimental approach*

124 *2.2.1 Starting composition*

125 We have conducted nominally anhydrous piston cylinder experiments on an Fe-
126 rich model basalt composition synthetic starting material (**Table 1**). The choice of the
127 basalt composition was motivated by the fact that the same composition had previously
128 been used to study the effect of chlorine on near-liquidus phase equilibria (Filiberto and
129 Treiman, 2009a). The synthetic starting material was made from reagent grade oxides and
130 carbonates ground together under acetone in an automatic mortar and pestle for 15
131 minutes to ensure homogeneity (Filiberto et al., 2008). This powdered mix was melted in
132 an iron-saturated Pt crucible in a muffle furnace at 1500°C under air, quenched to a glass,
133 and reground for 15 minutes. The same powder and experimental techniques from our
134 previous work was used for this study thus allowing comparisons between current and
135 past studies (Filiberto and Treiman, 2009a; Filiberto et al., 2008); however, 2.1 wt%
136 fluorine was added to the starting mix as AgF_2.

137 *2.2.2 Experimental Technique*

138 High pressure experiments were conducted in a non-end-loaded QuickPress©
139 piston-cylinder apparatus at Johnson Space Center High Pressure Laboratory. Standard
140 methods were employed. Starting materials were held in graphite sample capsules, which
141 were installed in straight graphite furnaces, insulated with $BaCO_3$ sleeves and crushable
142 MgO spacers (Filiberto et al., 2008). Before each run, the synthetic powder plus AgF_2
143 was loaded into a graphite capsule and stored for at least 12 hours in an oven at 150 °C in
144 order to drive off absorbed H_2O. Temperature was measured using a W5%Re/W25%Re
145 thermocouple placed in an indentation in the graphite sample capsule and range from

above the liquidus to just below the liquidus. Pressure in the experiments was measured on a Heise gauge and corrected for friction by -0.3 kbar based on the location of the diopside melting curve (Filiberto et al., 2008). Pressures in these experiments ranged from 5.7 kbar to 14.7 kbar and friction corrected pressures are reported (**Table 2**). The oxygen fugacity, fO_2, of our experiments has not been directly measured. However, the graphite capsules constrain the fO_2 of the assemblage, at elevated pressures, to ~1-2 log units below the FMQ oxygen buffer (Frost and Wood, 1995; Médard et al., 2008).

Experiments were conducted using a piston-out procedure – the experiment was pressurized cold to 2 kbar above the experimental pressure, brought to the desired temperature, and then brought down to the final pressure. Samples were kept for 30 minutes above the liquidus temperature, rapidly cooled to the final crystallization temperature where they remained for at least one hour, and finally quenched at pressure. This technique was employed in order to mimic natural magmatic conditions where crystals form directly from a molten liquid, rather than synthesis techniques of going directly to the crystallization temperature where crystals form from the powder.

In order to determine mineral abundances and verify that the experiments were chemically closed systems, mass balance calculations were conducted using the average starting bulk composition (**Table 1**) and the compositions of the crystallized phases and residual glass (**Table 3**), using the least square computations of the IgPet software package (Carr, 2000).

2.3 Chemical Analyses

2.3.1 Major Element Analyses

Experimental run products, glasses and crystalline phases, were analyzed for major and minor element abundances using the Cameca SX-100 electron microprobe at the NASA Johnson Space Center. Analytical conditions were 15 kV accelerating potential and focused electron beam of 20 nA current for minerals, and 15 kV electron accelerating potential and a defocused 5 μm electron beam of 10 nA current for quenched glasses. Analytical standards were synthetic oxides and minerals for minerals and natural and synthetic glasses for glasses.

2.3.2 F analysis

Glass in experimental run products was analyzed for dissolved F using a Cameca IMS 1280 ion probe at the Woods Hole Oceanographic Institution. Analytical standards were well characterized basaltic glasses. Experimental and standard samples were mounted in indium and gold-coated for analysis. The $^{19}F/^{30}Si$ ratio was measured by the ion probe, and F abundances were calculated using Si abundances measured by EMP (Helo et al., 2011). Replicate analyses were done on each sample to gauge precision, and an analytical uncertainty of ~10% of the measured abundance of F reflects uncertainties from counting statistics, and standard compositions (Table 2). Because the basaltic standards had lower F concentrations than our experimental sample glasses, a linear extrapolation of the calibration curve was adopted (e.g., Helo et al., 2011).

2.3.3 H_2O and CO_2 analyses

Because small amounts of dissolved water can have large effects on basalt liquidus temperatures (e.g., Almeev et al., 2007; Danyushevsky, 2001; Médard and Grove, 2008) and because performing completely dry but other volatile-bearing experiments is practically impossible, micro-FTIR analyses were conducted to determine

192 the water contamination of the experimental glasses. Samples were analyzed using a
193 Nicolet Contiuum FTIR in the geochemistry laboratory at Rice University. Total
194 dissolved water contents were determined on doubly polished glass wafers from the
195 intensity of the broad band at 3570 cm^{-1}. Each doubly polished wafer was measured for
196 thickness using a Mitutoyo electronic indicator with a 0.015″ carbine needlepoint tip. For
197 each sample 512 scans were used to acquire each IR spectrum. Density of the glass was
198 calculated from the bulk composition using the procedure of Dixon et al. (1995). A molar
199 absorptivity value of 65 (L/mol-cm) was applied (King et al., 2004). Total water
200 concentrations are reported in **Table 3**. They were calculated using the total H_2O
201 vibration band at 3550 cm^{-1} and the procedures of Dixon et al. (1995) and King et al.
202 (2004).

203 Because the starting material for our experiments was not reduced prior to the
204 high-pressure experiments, our experimental glasses were expected to suffer
205 contamination by small amount of CO_2, owing to reduction of Fe^{3+} to Fe^{2+} by reaction
206 with graphite. Micro-FTIR analysis was used to determine the dissolved CO_3^{2-} contents
207 of our experimental glasses. For each sample 512 scans were used to acquire each IR
208 spectrum. Density was of the glass was calculated from the bulk composition using the
209 procedure of Dixon et al. (1995). Total CO_3^{2-} concentrations were calculated using molar
210 absorptivity values of 284 and 281 (L/mol-cm) for the carbonate ion vibration band at
211 1515 and 1430 cm^{-1} respectively (King et al., 2004) and the procedures of Dixon et al.
212 (1995) and King et al. (2004).
213
214

3. Results

The FTIR spectra, for representative sample Hf18, shows peaks for both dissolved H_2O and CO_3^{2-} (**Figure 2**) representing volatile contamination in our experiments. The fluorine-bearing experiments contain an average of 0.34±0.07 wt. % H_2O. Selected samples analyzed for dissolved carbon show that the CO_2 contaminations are more scattered and give approximate average dissolved CO_2 contents of 0.53±0.28 wt. % (**Table 3**).

Figure 3 shows the near-liquidus phase diagram for the F-bearing basaltic composition in *P-T* space. Above 12 kbar, pigeonite is the liquidus phase; below 10 kbar, olivine is on the liquidus. At approximately 10 kbar and 1265 °C, the bulk composition with ~2 wt.% fluorine is multiply saturated with both olivine (Fo_{67}) and pigeonite ($En_{64}Wo_7Fs_{29}$). In the *P-T* range of our experiments, the olivine composition spans the range from Fo_{67} near the liquidus to Fo_{58} at lower temperatures. The pyroxenes are all pigeonite, and range from $En_{67}Wo_7Fs_{26}$ near the liquidus through $En_{57}Wo_{12}Fs_{30}$ at lower temperatures.

4. Discussion

4.1 Liquidus depression effect of Fluorine

Liquidus temperatures (at a given pressure) determined in this study for the F-bearing composition, are systematically lower than those of the F-free composition investigated earlier (Filiberto et al., 2008). However, quantification of the basalt liquidus depression effect of fluorine requires comparing all the data at the same background volatile content level. The fluorine-bearing experiments in our study contain more water

238 contamination (~0.34 wt% H_2O; **Table 3**) than the previous fluorine free experiments
239 (~0.1 wt% H_2O; Filiberto et al. 2008) and water is known to depress the liquidus
240 temperature (e.g., Médard and Grove, 2008); therefore, in order to make a direct
241 comparison, temperatures of all experiments need to be corrected to a water-free system,
242 i.e.,

243 $$\Delta T\ (\ ^\circ C)^{F} = \Delta T\ (\ ^\circ C)^{Total} - \Delta T\ (\ ^\circ C)^{H_2O} \quad (1)$$

244 where $\Delta T\ (\ ^\circ C)^{F}$ is the liquidus temperature depression caused by fluorine only, ΔT
245 $(^\circ C)^{H_2O}$ is the liquidus temperature depression caused by water only and $\Delta T\ (\ ^\circ C)^{Total}$ is
246 the total liquidus temperature depression observed in our experiments. In equation (1), we
247 assume that the liquidus depression effects of water and fluorine are additive. To
248 calculate $\Delta T\ (\ ^\circ C)^{H_2O}$ we use the liquidus depression equation from Médard and Grove
249 (2008)

250 $$\Delta T\ (\ ^\circ C)^{H_2O} = 40.4\ (C_{melt}{}^{H2O}) - 2.97\ (C_{melt}{}^{H2O})^2 + 0.0761\ (C_{melt}{}^{H2O})^3] \quad (2)$$

251 and add the calculated $\Delta T\ (\ ^\circ C)^{H_2O}$ to all of our experimental temperatures. Uncorrected
252 and corrected temperatures (T*) are reported in **Tables 2** but all temperatures used in
253 **Figures 4-7** are corrected for dissolved water and hence reflect the estimated
254 temperatures of the experimental assemblages if no water was present in the experiments.

255 No correction has been applied to account for the small amount of dissolved CO_2
256 because it likely has no discernable effect on the liquidus temperature of our experiments.
257 Brey and Green (1977; 1976) estimated the effect of dissolved CO_2 on the high pressure
258 liquidus temperature of olivine melilitite. Their study indicates that ~0.5 wt% dissolved
259 CO_2 (as carbonate) at 3 GPa lowers the liquidus of olivine melilitite, an extremely silica-
260 undersaturated magma, by less than 10-15 °C. The effect of CO_2 at lower pressures (this

261 study) and for more silica-rich basalt compositions will be even less pronounced (<< 10
262 °C).

263 We assume that the effects of different volatiles, i.e., H_2O and halogens on
264 liquidus depression are additive (equation 1). In order to test this assumption, we
265 calculated the expected liquidus depression for basalt from the study of McCubbin et al.
266 (2008). The basalt composition from the study of McCubbin et al. (2008) is similar to the
267 bulk composition from our experiments (this work, Filiberto and Treiman, 2009a;
268 Filiberto et al., 2008) but with two important differences – (1) their experiments were
269 doped with H_2O, Cl, and F and (2) their bulk composition contained Cr, therefore, had
270 chromite as the liquidus phases. Because our experiments were conducted Cr-free, we
271 ignored possible effect of chromite and considered the Ol-Pyx liquidus only. In their
272 study, experiments were conducted at 9.3 kbar with two different bulk compositions – (1)
273 0.07 wt% H_2O, 0.56 wt% F, and 0.15 wt% Cl and (2) 1.67 wt% H_2O, 0.55 wt% F, and
274 0.21 wt% Cl, respectively (McCubbin et al., 2008). For the effect of H_2O on the liquidus
275 depression we use equation 2 from Médard and Grove (2008), for the effect of F and Cl
276 on liquidus depression we use the results from our experiments (equation 3 below). For
277 bulk composition 1, starting from the volatile-free solidus of Filiberto et al. (2008), we
278 calculate an ol-opx liquidus temperature of 1300 °C at 9.3 kbar whereas the actual
279 experimental results have an ol-opx liquidus temperature of 1260 +/-10 °C at 9.3 kbar
280 (McCubbin et al., 2008). Similarly, for bulk composition 2, the actual experimental
281 results have an ol-opx liquidus temperature of 1225 +/- 25 °C (McCubbin et al., 2008)
282 whereas we estimated a temperature of 1240 °C. This shows the validity of the
283 assumption that basalt liquidus depression caused by a mixed halogen-water can be

within error approximated by the addition of the effect of individual species. The good reproduction of the McCubbin et al. (2008) liquidus suggests that at least for similar bulk and volatile composition this approach may be reasonable.

Figure 4 compares the pressure-temperature phase relations for the F-bearing experiments and the F-free experiments (Filiberto et al. 2008) after their nominal temperatures have been corrected for dissolved water. It is apparent from **Figure 4** that fluorine has a significant and large effect on the liquidus position and phase boundaries in basaltic system. Addition of ~2 wt.% F moves the olivine-pigeonite liquidus point down ~2 kbar and 95 °C (from 12 kbar and 1375 °C to 10 kbar and 1280 °C) by expanding the stability field of pigeonite to lower pressure compared to the F-free experiments. We note that although we feel confident about correcting for the variable amount of water for the basalt liquidus when olivine is the sole liquidus phase, such correction for higher pressure experiments, i.e., with pigeonite as the liquidus phase, is less certain. This is because the liquidus depression effect of water on the liquidus of pigeonite is not constrained for composition similar to that explored in our study.

4.2 Fluorine Complexation in the Melt and Compositions of Crystallizing Phases

In order to constrain how fluorine is complexing in the melt, we can investigate the effect of dissolved fluorine on Fe-Mg partitioning between minerals and melt ($Kd^{Fe-Mg}_{Mineral-Melt} = [X_{FeO}{}^{(ol,\ pig)}X_{MgO}{}^{L}]/[X_{MgO}{}^{(ol,pig)}X_{FeO}{}^{L}]$). **Figure 5** shows $Kd^{Fe-Mg}_{Mineral-Melt}$ for both olivine and pyroxene compared with the wt.% fluorine in the melt as analyzed by SIMS. With increasing fluorine concentrations, $Kd^{Fe-Mg}_{Mineral-Melt}$ dramatically increases for both pyroxene and olivine, suggesting that fluorine in the basaltic magma is complexing

with MgO over FeO in the melt. Complexing with MgO in the melt will decrease the MgO activity in the melt and force the minerals crystallizing to be more ferroan (higher Fe/Mg) than they would be without fluorine in the melt. Our results are thus consistent with NMR studies, which suggest the presence of Mg-F complexes in fluorine bearing aluminosilicate glasses (Kiczenski et al., 2004). However, the nature of the F-cation complexes is likely highly compositionally dependent (Liu and Nekvasil, 2002; Liu and Tossell, 2003; Luth, 1988b; Schaller et al., 1992; Zeng et al., 1999; Zeng and Stebbins, 2000). Therefore, the effect of fluorine on liquidus depression and mineral crystallization will depend on the melt composition and we caution the readers against applying our liquidus depression parameterization to other melt compositions.

4.3 Fluorine Solubility

The results here can also help to constrain our understanding of fluorine solubility in basaltic magmas. There is limited experimental data for fluorine solubility in magmas (for a review see Carroll and Webster, 1994). What experimental data there is for Si-rich magmas is mainly at low pressure and low temperature (Dolejs and Baker, 2007a; Dolejs and Baker, 2007b; Mysen et al., 2004; Scaillet and Macdonald, 2004; Webster, 1990). For example, $NaAlSi_3O_8$ magma compositions can contain up to ~20 wt% F at 15 Kbar, Ca-poor peralkaline rhyolitic melts can contain up to 4.28 wt% at 1 bar, and rhyolitic magma at pressures from 0.5-5 kbar can contain up to 8.5 wt% F (for a review see, Carroll and Webster, 1994; Scaillet and Macdonald, 2004; Webster, 1990). In natural carbonatitic melts, F content of up to 16 wt. % have been reported and in carbonated silicate melts of kimberlitic/melilititc affinity, F content of as much as 13 wt.% have been measured (Brey et al., 2009). Therefore, F solubility is likely compositionally dependent

and there is currently no experimental solubility data on natural basaltic magmas at pressure. The results here present constraints on the lower solubility limit of F in Fe-Mg-rich basaltic magmas at 5.7-11.7 kbar pressure. Because the magmas are not in equilibrium with fluorite, these results are only a minimum for the solubility. The glass in these experiments contain up to 2.89 wt. % suggesting that the F solubility in basaltic magmas are higher than this value.

4.4 Comparison to the effects of chlorine

Experiments have been previously conducted on the same bulk composition used in this study to investigate the effect of chlorine on near-liquidus equilibria (Filiberto and Treiman, 2009a). Therefore, we can directly compare the effect of fluorine and chlorine on liquidus depression and $Kd^{Fe-Mg}_{Mineral-Melt}$ on the same bulk composition. **Figure 6** shows the effect of dissolved volatile contents (Cl and F) on liquidus depression (a) and $Kd^{Fe-Mg}_{Mineral-Melt}$ (b). These results show that for the pressures, temperatures, and compositions studied, fluorine and chlorine have similar effects on liquidus depression and a single power curve can be fit through the data to explain both data sets (equation 3).

$$\Delta T\ (^{\circ}\mathrm{C}) = 46.737(\mathrm{C}_{\mathrm{melt}}{}^{\text{F or Cl}}\ \text{in wt\%})^{0.6263} \qquad (3)$$

However, fluorine and chlorine have opposite effects on $Kd^{Fe-Mg}_{Mineral-Melt}$. Fluorine increases $Kd^{Fe-Mg}_{Mineral-Melt}$ because it complexes mainly with Mg whereas chlorine decreases $Kd^{Fe-Mg}_{Mineral-Melt}$ because it complexes mainly with Fe (Filiberto and Treiman, 2009a).

Because F and Cl likely form different ion-complexes in the melt, a single power curve fitting for both data sets in Figure 6a is surprising and likely coincidental.

4.5 Comparison to the effects of water

In order to compare these results to the effect of water, we rely on experiments and models of the effect of water on liquidus depression conducted on varying basaltic bulk compositions over a range of pressures (0.1-10 kbar), temperatures (1350-1130 °C), water contents (0-11.5 wt.%), and approaches (Almeev et al., 2007; Ghiorso et al., 2002; Katz et al., 2003; Médard and Grove, 2008). **Figure 6** shows the effect of volatile contents (H_2O, Cl, and F) on ΔT (°C), the depression of the liquidus temperature. It appears that the effect of increasing H_2O, Cl and F on basalt liquidus depression can be parameterized with similar function when compared on a weight percent basis. While analyzing and reporting Cl, F, and H_2O in weight percent basis are the routine geochemical practice, to compare the freezing point depression effect of F, Cl and H_2O on a more thermodynamically rigorous basis, it is more desirable to compare liquidus depression based on the atomic fraction of F, Cl and H. On an atomic fraction basis, F and Cl are actually 2-3 times more efficient at liquidus depression than H (**Figure 7**).

The effects of dissolved Cl, F, and H_2O on $Kd^{Fe-Mg}_{Mineral-Melt}$ are rather dissimilar which suggests that these species have different solution mechanisms, i.e. are sited differently in silicate magmas. Dissolved F increases $Kd^{Fe-Mg}_{Mineral-Melt}$, dissolved Cl decreases $Kd^{Fe-Mg}_{Mineral-Melt}$, and dissolved H_2O has no discernible effect on $Kd^{Fe-Mg}_{Mineral-Melt}$ (Figure 6, Filiberto and Treiman, 2009a; Gaetani and Grove, 1998; Médard and Grove, 2008; Whitaker et al., 2008). This is consistent with complexation of F and Cl with divalent 'network-

modifying' cations while H_2O does not complex with 'network-modifying' cations at all but bonds dominantly with Al (e.g., Burnham and Davis, 1974; Giordano et al., 2004).

5. Implications

Fluorine has a large effect on liquidus depression of basalts and the chemistry of crystallizing minerals; these effects will be especially important for low-degree partial melts, which may start with relatively high abundances of fluorine. If we extrapolate these experimental results to alkalic magma compositions (terrestrial or martian) with up to 5000 ppm F (likely derived from a F-rich source and/or as a result of very low-extent of melting; **Figure 1**), liquidus temperature can be depressed by an extra ~30°C which is not accounted for by dissolved water alone. If this can be further extrapolated to mantle temperatures, a ~30 °C shift in temperature, with a shift in ol:pyx stability field as well, enables alkalic melts to be produced at lower temperatures. This suggests that fluorine may significantly aid in the petrogenesis of silica-poor, alkali-rich magmas in the Earth and Mars. Because martian magmas can be more F-rich, it is perhaps more appropriate to further comment on the effect of fluorine on the multiple saturation point of olivine-opx-melt in martian igneous system. With average F content of ~5000 ppm, our present study suggests that the mantle potential temperatures relevant for Mars can be as low as 1335-1495 °C, distinctly lower than a recent estimate based on olivine-melt Mg-exchange thermometry (Filiberto and Dasgupta, 2011).

Acknowledgements- We thank an anonymous reviewer as well as associate editor Don Dingwell for helpful comments. We are grateful to Peter Luffi for help with the FTIR. This work was supported by NASA MFR grant # NNX09AL25G to A.H. Treiman

397 and J. Filiberto, a Lunar and Planetary Institute summer internship to J. Wood, and a
398 Packard fellowship for science and engineering to R. Dasgupta. LPI contribution # 1664.
399

Figure Captions:

Figure 1. Plausible concentration of fluorine in near-solidus partial melts of garnet peridotite as a function of melting degree for Earth (bulk F concentration from McDonough and Sun, 1995) and Mars (assuming that martian mantle contains three times F than that in the Earth's mantle). Bulk partition coefficient, D_F (peridotite-basalt), of 0.0785 is used based on olivine-melt D_F of 0.1164, opx-melt D_F of 0.0158, cpx-melt D_F of 0.0428, and garnet-melt D_F of 0.0123 from the study of Dalou et al. (2012). Garnet-melt, opx-melt, and cpx-melt D_F values are taken from the experiment C4p#25kb and that of olivine-melt D_F from the experiment CC01#8kb4 of Dalou et al. (2012). Peridotite mineral modes used for the calculations are 60% olivine, 20% opx, and 10% each of cpx and garnet. Because of the uncertainties in D_F (mineral-melt) for Martian mantle phase compositions, melt compositional trends for $D_F = 0$ are also shown for reference.

Figure 2. Representative FTIR spectrum of sample Hf18 showing distinct peaks for total H_2O and CO_3^{2-} peaks.

Figure 3. Experimentally determined near-liquidus phase relations for synthetic basaltic composition with 2.17 wt% F.

Figure 4. Experimentally determined near-liquidus phase relations for synthetic basaltic composition with 2.17 wt% F (black symbols) compared with nominally volatile-free (gray symbols) experiments (Filiberto et al., 2008). Both data sets are corrected for dissolved water in experimental glasses.

Figure 5. $Kd^{Fe-Mg}_{Mineral-Melt}$ as a function of F (wt%) for olivine-bearing (black circles) and pigenoite-bearing (open circles) experimental charges. Black lines represent linear

regressions through the data with R^2= 0.8890 for olivine and 0.9076 for pyroxene bearing experiments.

Figure 6. (a) Calculated liquidus depression (ΔT° in C) as a function of volatile element (F or Cl) content in the melt (wt%) for fluorine-bearing experiments (this study; circles) and chlorine-bearing experiments (squares) (Filiberto and Treiman, 2009a), compared with the calculated olivine-liquidus depression from previous studies (Almeev et al., 2007; Ghiorso et al., 2002; Katz et al., 2003; Médard and Grove, 2008). Experiments containing only liquid are shown by open symbols and those containing crystals (either olivine or pyroxene or both) are shown by closed symbols. All curves are fit through the origin. One sigma uncertainties in volatile concentrations are shown with error bars. Where error bars are not shown for chlorine concentrations, the 1σ uncertainty is smaller than the size of the symbol. **(b)** $Kd^{Fe-Mg}_{Mineral-Melt}$ as a function of volatile content (F, Cl, or H_2O) in the melt. Closed symbols represent olivine-liquidus experiments and open symbols represent pyroxene-liquidus experiments. Data for water-bearing experiments (diamonds) from: Gaetani and Grove (1998, gray); Médard and Grove (2008, black); Whitaker et al. (2008, white), regression shown for all data (black solid line).

Figure 7. Calculated liquidus depression (ΔT in °C) as a function of the atomic fraction of volatile species (F, Cl, H) in the melt for containing fluorine-bearing experiments (this study; circles) compared with previous chlorine-bearing experiments (squares) (Filiberto and Treiman, 2009a) and H-bearing olivine-liquidus experiments (triangles; Almeev et al. 2007) and (diamonds; Médard and Grove 2008). Experiments containing only liquid are shown by open symbols and those containing crystals (either olivine or pyroxene or both) are shown by closed symbols. All curves are fit through the origin.

References

Almeev, R.R., Holtz, F., Koepke, J., Parat, F., Botcharnikov, R.E., 2007. The effect of H_2O on olivine crystallization in MORB: Experimental calibration at 200 MPa. American Mineralogist, 92: 670-674.

Aoki, K., Ishiwaka, K., Kanisawa, S., 1981. Fluorine geochemistry of basaltic rocks from continental and oceanic regions and petrogenetic application. Contributions to Mineralogy and Petrology, 76(1): 53-59.

Brey, G., Green, D.H., 1977. Systematic study of liquidas phase relations in olivine melilitite +H2O +CO2 at high pressures and petrogenesis of an olivine melilitite magma. Contributions to Mineralogy and Petrology, 61(2): 141-162.

Brey, G.P., Bulatov, V.K., Girnis, A.V., 2009. Influence of water and fluorine on melting of carbonated peridotite at 6 and 10 GPa. Lithos, 112(Supplement 1): 249-259.

Brey, G.P., Green, D.H., 1976. Solubility of CO2 in olivine melilitite at high pressures and role of CO2 in the earth's upper mantle. Contributions to Mineralogy and Petrology, 55(2): 217-230.

Burnham, C.W., Davis, F.A., 1974. The role of H_2O in silicate melts II: Thermodynamic and phase relations in the system $NaAlSi_3O_8$-H_20 to 10 kilobars, 700^o to 1000^oC. American Journal of Science, 274: 902-940.

Carr, M.J., 2000. Igpet for Windows. Terra Softa Inc., Somerset, N.J.

Carroll, M.R., Webster, J.D., 1994. Solubilities of sulfur, noble gases, nitrogen, chlorine, and fluorine in magmas. In: Carroll, M.R., Webster, J.D. (Eds.), Volatiles in Magmas. Reviews in Mineralogy. Mineralogical Society of America, Washington, D.C., pp. 231-279.

Dalou, C., Koga, K., Shimizu, N., Boulon, J., Devidal, J.-L., 2012. Experimental determination of F and Cl partitioning between lherzolite and basaltic melt. Contributions to Mineralogy and Petrology: 10.1007/s00410-011-0688-2.

Danyushevsky, L.V., 2001. The effect of small amounts of H_2O on crystallisation of mid-ocean ridge and backarc basin magmas. Journal of Volcanology and Geothermal Research, 110(3): 265-280.

Dasgupta, R., Hirschmann, M., Smith, N., 2007. Partial melting experiments of peridotite + CO2 at 3 GPa and genesis of alkalic ocean island basalts. Journal of Petrology, 48(11): 2093-2124.

Dingwell, D.B., 1989. Effect of fluorine on the viscosity of diopside liquid. American Mineralogist, 74(3-4): 333-338.

480 Dingwell, D.B., Hess, K.U., 1998. Melt viscosities in the system Na-Fe-Si-OF-Cl;
481 contrasting effects of F and Cl in alkaline melts. American Mineralogist, 83(9-
482 10): 1016-1021.

483 Dingwell, D.B., Scarfe, C.M., Cronin, D.J., 1985. The effect of fluorine on viscosities in
484 the system Na_2O-Al_2O_3 SiO_2; implications for phonolites, trachytes and rhyolites.
485 American Mineralogist, 70(1-2): 80-87.

486 Dixon, J.E., Stolper, E.M., Holloway, J.R., 1995. An Experimental Study of Water and
487 Carbon Dioxide Solubilities in Mid-Ocean Ridge Basaltic Liquids. Journal of
488 Petrology, 36(6): 1607-1631.

489 Dolejs, D., Baker, D.R., 2007a. Liquidus Equilibria in the System K_2O-Na_2O-Al_2O_3-
490 SiO_2-F_2O^{-1}-H_2O to 100 MPa: I. Silicate-Fluoride Liquid Immiscibility in
491 Anhydrous Systems. Journal of Petrology, 48(4): 785-806.

492 Dolejs, D., Baker, D.R., 2007b. Liquidus Equilibria in the System K_2O-Na_2O-Al_2O_3-
493 SiO_2-F_2O^{-1}-H_2O to 100 MPa: II. Differentiation Paths of Fluorosilicic Magmas in
494 Hydrous Systems. Journal of Petrology, 48(4): 807-828.

495 Dreibus, G., Wänke, H., 1985. Mars, a Volatile-Rich Planet. Meteoritics, 20(2): 367-381.

496 Dreibus, G., Wänke, H., 1987. Volatiles on Earth and Mars - a Comparison. Icarus,
497 71(2): 225-240.

498 Dunn, T.L., McSween, H.Y., Jr., Christensen, P.R., 2007. Thermal emission spectra of
499 terrestrial alkaline volcanic rocks: Applications to Martian remote sensing. J.
500 Geophys. Res., 112(E05001): doi:10.1029/2006JE002766.

501 Feig, S., Koepke, J., Snow, J., 2010. Effect of oxygen fugacity and water on phase
502 equilibria of a hydrous tholeiitic basalt. Contributions to Mineralogy and
503 Petrology, 160(4): 551-568.

504 Feig, S.T., Koepke, J., Snow, J.E., 2006. Effect of water on tholeiitic basalt phase
505 equilibria: an experimental study under oxidizing conditions. Contributions to
506 Mineralogy and Petrology, 152(5): 611-638.

507 Filiberto, J., Dasgupta, R., 2011. Fe^{2+}-Mg partitioning between olivine and basaltic melts:
508 Applications to genesis of olivine-phyric shergottites and conditions of melting in
509 the Martian interior. Earth and Planetary Science Letters, 304(3-4): 527-537.

510 Filiberto, J., Treiman, A.H., 2009a. The effect of chlorine on the liquidus of basalt: First
511 results and implications for basalt genesis on Mars and Earth. Chemical Geology,
512 263(1-4): 60-68.

513 Filiberto, J., Treiman, A.H., 2009b. Martian magmas contained abundant chlorine, but
514 little water. Geology, 37(12): 1087-1090.

Filiberto, J., Treiman, A.H., Le, L., 2008. Crystallization experiments on a Gusev Adirondack basalt composition. Meteoritics & Planetary Science, 43(7): 1137-1146.

Foley, S.F., Taylor, W.R., Green, D.H., 1986. The effect of fluorine on phase relationships in the system KAlSiO4-Mg2SiO4-SiO2 at 28 kbar and the solution mechanism of fluorine in silicate melts. Contributions to Mineralogy and Petrology, 93(1): 46-55.

Frost, D., Wood, B., 1995. Experimental measurements of the graphite C−O equilibrium and CO_2 fugacities at high temperature and pressure. Contributions to Mineralogy and Petrology, 121(3): 303-308.

Gaetani, G.A., Grove, T.L., 1998. The influence of water on melting of mantle peridotite. Contributions to Mineralogy and Petrology, 131(4): 323-346.

Gerbode, C., Dasgupta, R., 2010. Carbonate-fluxed Melting of MORB-like Pyroxenite at 2·9 GPa and Genesis
51(10): 2067-2088.

Ghiorso, M.S., Hirschmann, M.M., Reiners, P.W., Kress, V.C., 2002. The pMELTS: A revision of MELTS for improved calculation of phase relations and major element partitioning related to partial melting of the mantle to 3 GPa. Geochemistry Geophysics Geosystems, 3: 1030, doi:10.1029/2001GC000217

Giordano, D., Romano, C., Dingwell, D.B., Poe, B., Behrens, H., 2004. The combined effects of water and fluorine on the viscosity of silicic magmas. Geochimica et Cosmochimica Acta, 68(24): 5159-5168.

Green, D.H., 1970. A review of experimental evidence on the origin of basaltic and nephelinitic magmas. Physics of The Earth and Planetary Interiors, 3: 221-235.

Grove, T., Parman, S., Bowring, S., Price, R., Baker, M., 2002. The role of an H_2O-rich fluid component in the generation of primitive basaltic andesites and andesites from the Mt. Shasta region, N California. Contributions to Mineralogy and Petrology, 142(4): 375-396.

Grove, T.L., Chatterjee, N., Parman, S.W., Médard, E., 2006. The influence of H2O on mantle wedge melting. Earth and Planetary Science Letters, 249(1-2): 74-89.

Harms, E., Schmincke, H.U., 2000. Volatile composition of the phonolitic Laacher See magma (12900 yr BP): implications for syn-eruptive degassing of S, F, Cl, and H2O. Contributions to Mineralogy and Petrology, 138: 84-98.

Helo, C., Longpre, M.-A., Shimizu, N., Clague, D.A., Stix, J., 2011. Explosive eruptions at mid-ocean ridges driven by CO2-rich magmas. Nature Geosci, 4(4): 260-263.

550 Katz, R.F., Spiegelman, M., Langmuir, C.H., 2003. A new parameterization of hydrous
551 mantle melting Geochemistry Geophysics Geosystems, 4(9): 1073; DOI
552 10.1029/2002GC000433

553 Kiczenski, T.J., Du, L.-S., Stebbins, J.F., 2004. F-19 NMR study of the ordering of high
554 field strength cations at fluoride sites in silicate and aluminosilicate glasses.
555 Journal of Non-Crystalline Solids, 337(2): 142-149.

556 King, P.L., McMillian, P.F., Moore, G.M., 2004. INFRARED SPECTROSCOPY OF
557 SILICATE GLASSES WITH APPLICATION TO NATURAL SYSTEMS. In:
558 King, P.L., Ramsey, M.S., Swayze, G.A. (Eds.), Infrared Spectroscopy in
559 Geochemistry, Exploration Geochemistry and Remote Sensing. Mineralogical
560 Association of Canada, Short Course Series, pp. 93-133.

561 Liu, Y., Nekvasil, H., 2002. Si-F bonding in aluminosilicate glasses: Inferences from ab
562 initio NMR calculations. American Mineralogist, 87(2-3): 339-346.

563 Liu, Y., Tossell, J., 2003. Possible Al−F Bonding Environment in Fluorine-Bearing
564 Sodium Aluminosilicate Glasses: From Calculatio
565 Journal of Physical Chemistry B, 107(41): 11280-11289.

566 Lukkari, S., Holtz, F., 2007. Phase relations of a F-enriched peraluminous granite: an
567 experimental study of the Kymi topaz granite stock, southern Finland.
568 Contributions to Mineralogy and Petrology, 153(3): 273-288.

569 Luth, R.W., 1988a. Effects of F on phase equilibria and liquid structure in the system
570 $NaAlSiO_4$-$CaMgSi_2O_6$-SiO_2. American Mineralogist, 73(3-4): 306-312.

571 Luth, R.W., 1988b. Raman spectroscopic study of the solubility mechanisms of F in
572 glasses in the system CaO-CaF-SiO. American Mineralogist, 73: 297-305.

573 Mandeville, C.W. et al., 2002. Determination of molar absorptivities in infrared
574 absorption bands of H_2O in andesitic glasses. Am. Mineralogist, 87: 813-821.

575 Manning, D.A.C., 1981. The effect of fluorine on liquidus phase relationships in the
576 system Qz-Ab-Or with excess water at 1 kb. Contributions to Mineralogy and
577 Petrology, 76(2): 206-215.

578 McCubbin, F.M., Nekvasil, H., Harrington, A.D., Elardo, S.M., Lindsley, D.H., 2008.
579 Compositional diversity and stratification of the Martian crust: Inferences from
580 crystallization experiments on the picrobasalt Humphrey from Gusev Crater,
581 Mars,. Journal of Geophysical Research, 113(E11013):
582 doi:10.1029/2008JE003165.

583 McDonough, W.F., Sun, S.s., 1995. The composition of the Earth. Chemical Geology,
584 120(3-4): 223-253.

McSween, H.Y. et al., 2006. Alkaline volcanic rocks from the Columbia Hills, Gusev crater, Mars. J. Geophys. Res., 111(E9): E09S91.

Médard, E., Grove, T., 2008. The effect of H_2O on the olivine liquidus of basaltic melts: experiments and thermodynamic models. Contributions to Mineralogy and Petrology, 155(4): 417-432.

Médard, E., McCammon, C.A., Barr, J.A., Grove, T.L., 2008. Oxygen fugacity, temperature reproducibility, and H_2O contents of nominally anhydrous piston-cylinder experiments using graphite capsules. American Mineralogist, 93: 1838-1844.

Monders, A.G., Médard, E., Grove, T.L., 2007. Phase equilibrium investigations of the Adirondack class basalts from the Gusev plains, Gusev crater, Mars. Meteoritics & Planetary Science, 42(1): 131-148.

Mysen, B., 1975. Melting of hydrous mantle: I. Phase relations of natural peridotite at high pressures and temperatures with controlled activities of water, carbon dioxide and hydrogen. Journal of Petrology, 16(3): 520-548.

Mysen, B.O., Cody, G.D., Smith, A., 2004. Solubility mechanisms of fluorine in peralkaline and meta-aluminous silicate glasses and in melts to magmatic temperatures. Geochimica et Cosmochimica Acta, 68(12): 2745-2769.

Nekvasil, H. et al., 2004. The origin and evolution of silica-saturated alkalic suites: an experimental study. Journal of Petrology, 45(4): 693-721.

Nekvasil, H., Filiberto, J., McCubbin, F.M., Lindsley, D.H., 2007. Alkalic parental magmas for the chassignites? Meteoritics & Planetary Science, 42(6): 979-992.

Patiño Douce, A.E., Roden, M., 2006. Apatite as a probe of halogen and water fugacities in the terrestrial planets. Geochimica et Cosmochimica Acta, 70(12): 3173-3196.

Patiño Douce, A.E., Roden, M.F., Chaumba, J., Fleisher, C., Yogodzinski, G., 2011. Compositional variability of terrestrial mantle apatites, thermodynamic modeling of apatite volatile contents, and the halogen and water budgets of planetary mantles. Chemical Geology, 288(1-2): 14-31.

Scaillet, B., MacDonald, R., 2001. Phase Relations of Peralkaline Silicic Magmas and Petrogenetic Implications. Journal of Petrology, 42(4): 825-845.

Scaillet, B., MacDonald, R., 2003. Experimental Constraints on the Relationships between Peralkaline Rhyolites of the Kenya Rift Valley. Journal of Petrology, 44(10): 1867-1894.

Scaillet, B., Macdonald, R., 2004. Fluorite stability in silicic magmas. Contributions to Mineralogy and Petrology, 147(3): 319-329.

Scaillet, B., Macdonald, R., 2006. Experimental constraints on pre-eruption conditions of pantelleritic magmas: Evidence from the Eburru complex, Kenya Rift. Lithos, 91(1-4): 95-108.

Schaller, T. et al., 1992. Fluorine in silicate glasses: A multinuclear nuclear magnetic resonance study. Geochimica et Cosmochimica Acta, 56(2): 701-707.

Stecher, O., 1998. Fluorine geochemistry in volcanic rock series: examples from Iceland and Jan Mayen. Geochimica et Cosmochimica Acta, 62(18): 3117-3130.

Treiman, A.H., Drake, M.J., Janssens, M.-J., Wolf, R., Ebihara, M., 1986. Core formation in the Earth and Shergottite Parent Body (SPB): Chemical evidence from basalts. Geochimica et Cosmochimica Acta, 50(6): 1071-1091.

Webster, J.D., 1990. Partitioning of F between H_2O and CO_2 fluids and topaz rhyolite melt. Contributions to Mineralogy and Petrology, 104(4): 424-438.

Webster, J.D., Thomas, R., Rhede, D., Förster, H.-J., Seltmann, R., 1997. Melt inclusions in quartz from an evolved peraluminous pegmatite: Geochemical evidence for strong tin enrichment in fluorine-rich and phosphorus-rich residual liquids. Geochimica et Cosmochimica Acta, 61(13): 2589-2604.

Weidner, J.R., Martin, R.F., 1987. Phase equilibria of a fluorine-rich leucogranite from the St. Austell pluton, Cornwall. Geochimica et Cosmochimica Acta, 51(6): 1591-1597.

Whitaker, M., Nekvasil, H., Lindsley, D., McCurry, M., 2008. Can crystallization of olivine tholeiite give rise to potassic rhyolites?—an experimental investigation. Bulletin of Volcanology, 70(3): 417-434.

Xiao-lin, X., Zhenhua, Z., Jinchu, Z., Bing, R., 1999. Phase relations in albite granite-H_20-HF system and their petrogenetic applications. Geochemical Journal, 33(3): 199-214.

Xiong, X.-L., Rao, B., Chen, F.-R., Zhu, J.-C., Zhao, Z.-H., 2002. Crystallization and melting experiments of a fluorine-rich leucogranite from the Xianghualing Pluton, South China, at 150 MPa and H2O-saturated conditions. Journal of Asian Earth Sciences, 21(2): 175-188.

Yoshida, M., Takahashi, K., Yonehara, N., Ozawa, T., Iwasaki, I., 1971. FLUORINE, CHLORINE, BROMINE, AND IODINE CONTENTS OF VOLCANIC ROCKS IN JAPAN. Bulletin of the Chemical Society of Japan, 44(7): 1844-1850.

Zeng, Q., Nekvasil, H., Grey, C.P., 1999. Proton environments in hydrous aluminosilicate glasses: A H-1 MAS, H-1/Al-27, and H-1/Na-23 TRAPDOR NMR study. Journal of Physical Chemistry B, 103(35): 7406-7415.

655 Zeng, Q., Stebbins, J.F., 2000. Fluoride sites in aluminosilicate glasses; high-resolution
656 19 F NMR results. American Mineralogist, 85(5-6): 863-867.

657 Zimova, M., Webb, S.L., 2007. The combined effects of chlorine and fluorine on the
658 viscosity of aluminosilicate melts. Geochimica et Cosmochimica Acta, 71(6):
659 1553-1562.
660
661

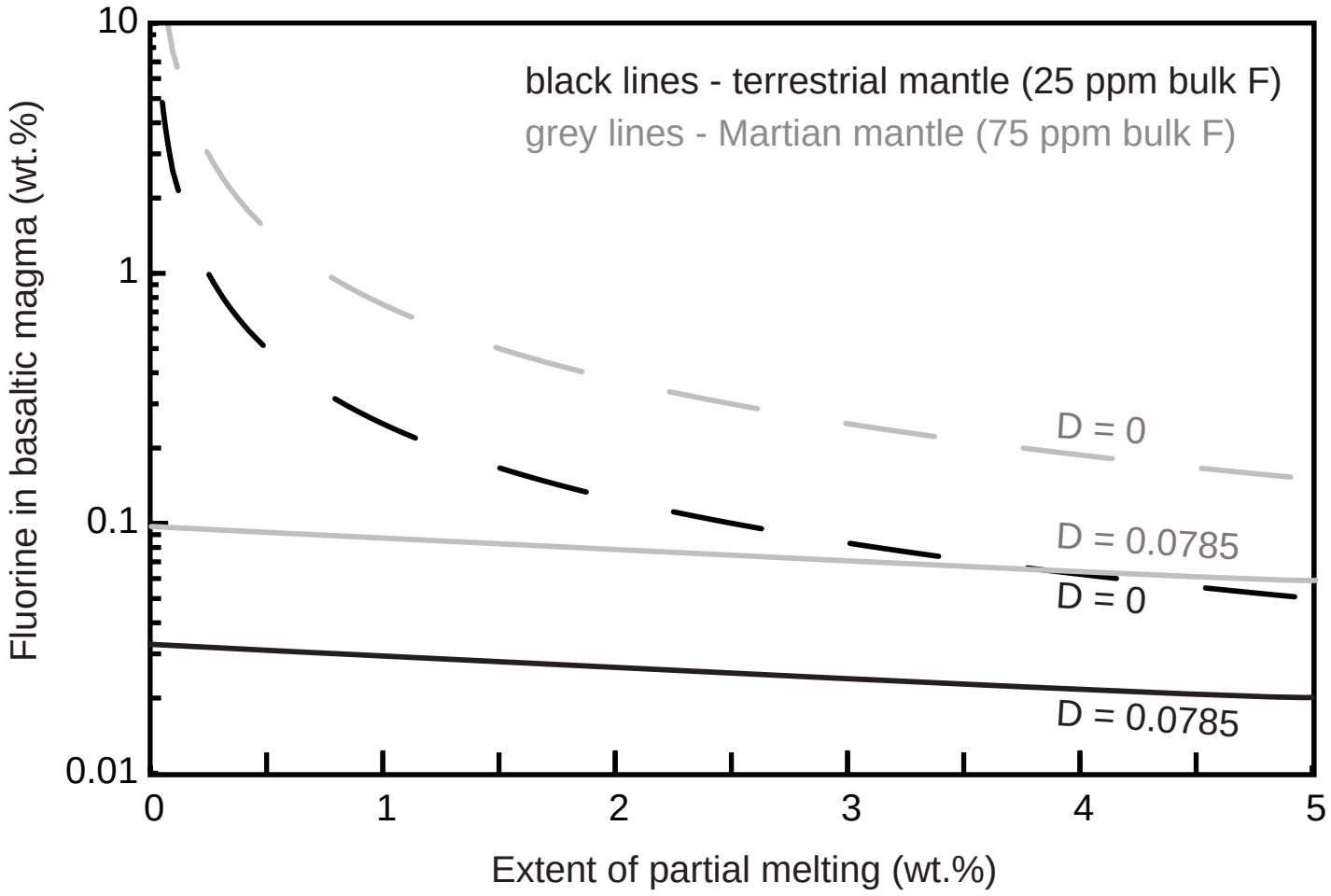
black lines - terrestrial mantle (25 ppm bulk F)
grey lines - Martian mantle (75 ppm bulk F)
D = 0
D = 0.0785
D = 0
D = 0.0785
Fluorine in basaltic magma (wt.%)
10
1
0.1
0.01
0
1
2
3
4
5
Extent of partial melting (wt.%)

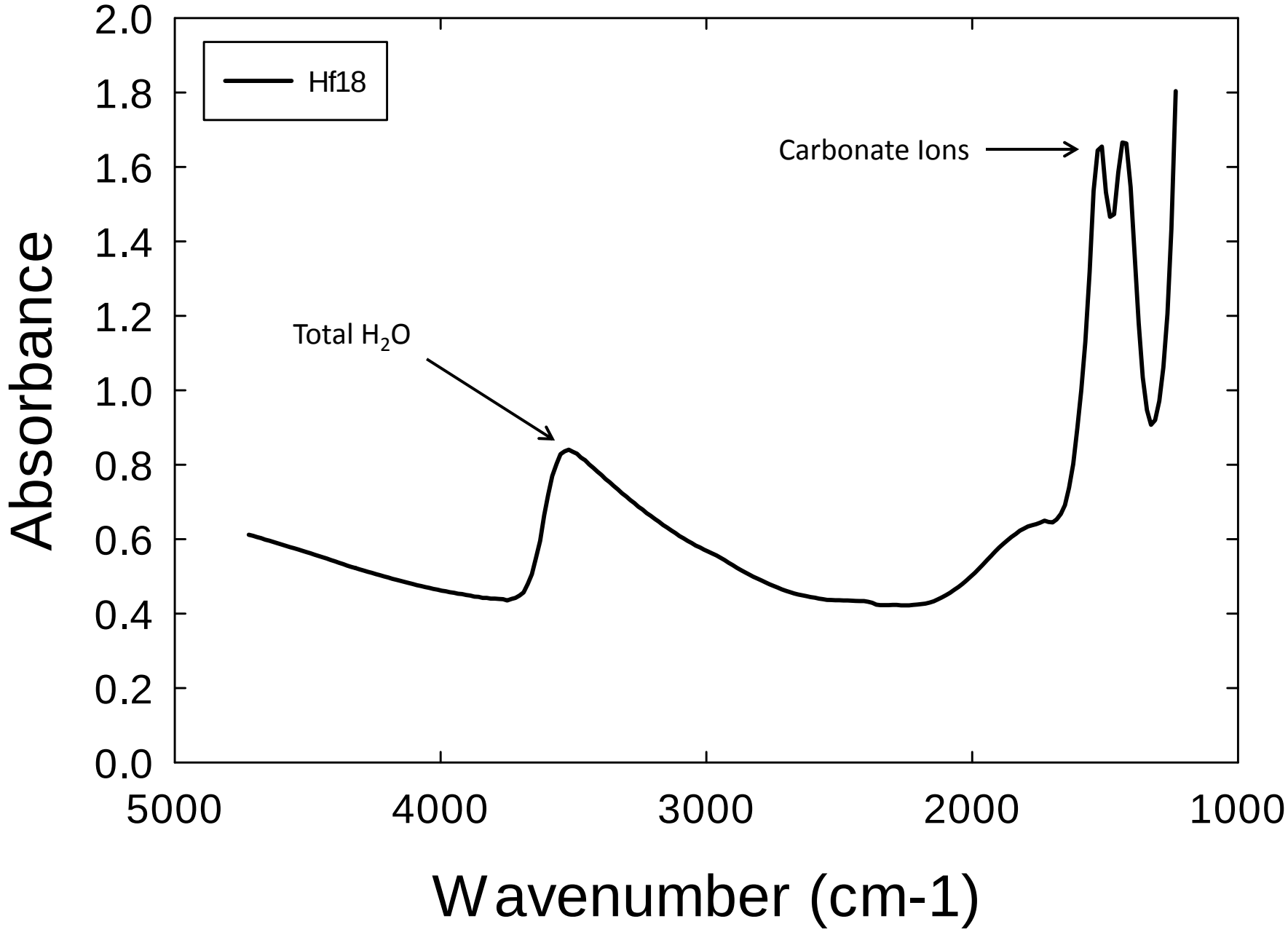
Hf18
Carbonate Ions
Total H_2O
Absorbance
Wavenumber (cm-1)
2.0
1.8
1.6
1.4
1.2
1.0
0.8
0.6
0.4
0.2
0.0
5000
4000
3000
2000
1000

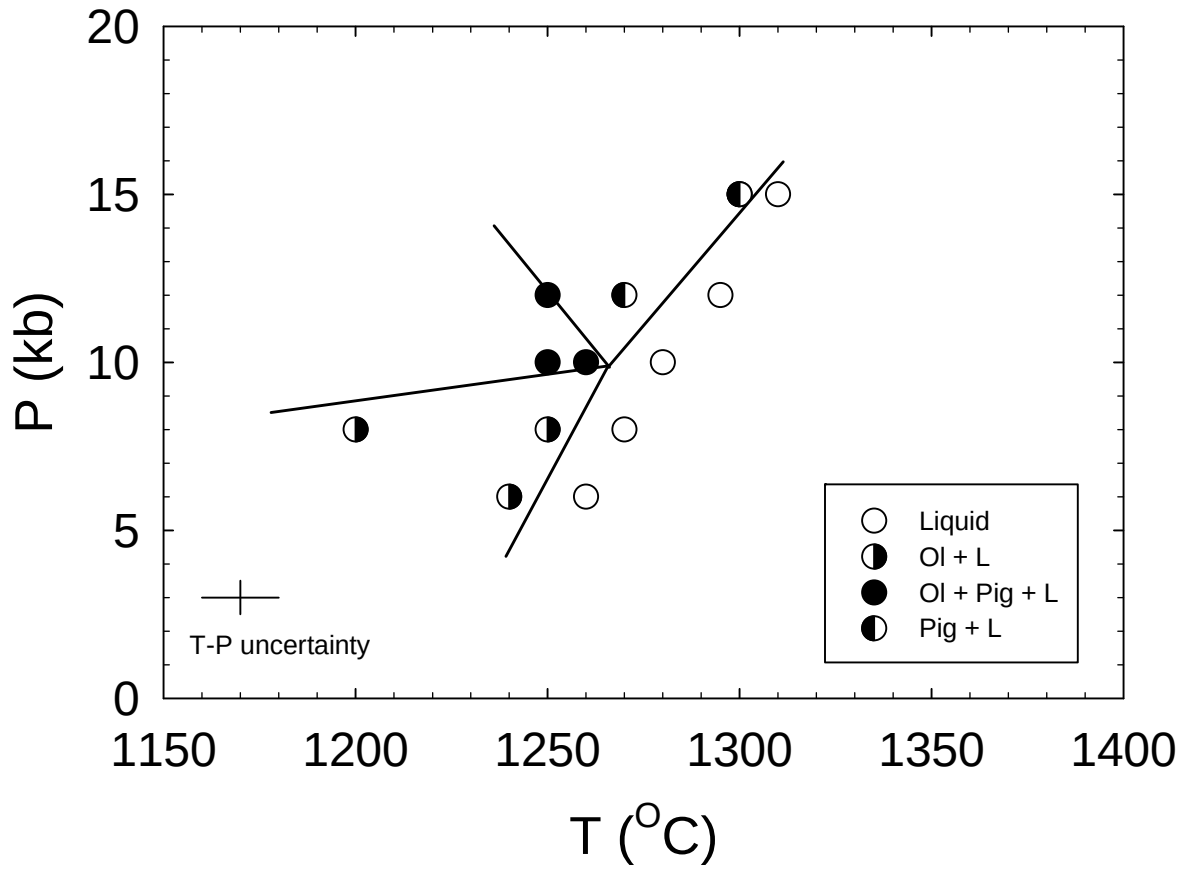
20
15
10
5
0
P (kb)
1150
1200
1250
1300
1350
1400
T (°C)
Liquid
Ol + L
Ol + Pig + L
Pig + L
T-P uncertainty

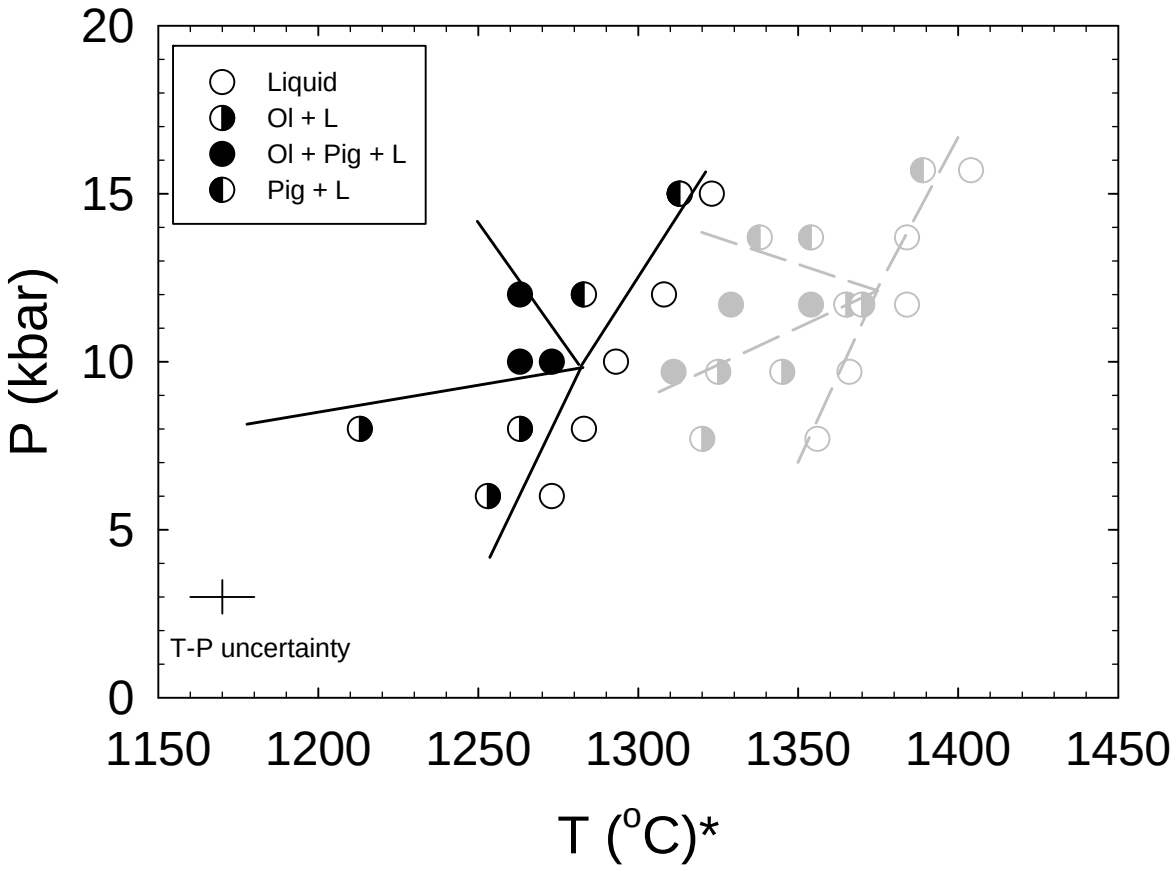
Liquid
Ol + L
Ol + Pig + L
Pig + L
T-P uncertainty
P (kbar)
T (°C)*
0
5
10
15
20
1150
1200
1250
1300
1350
1400
1450

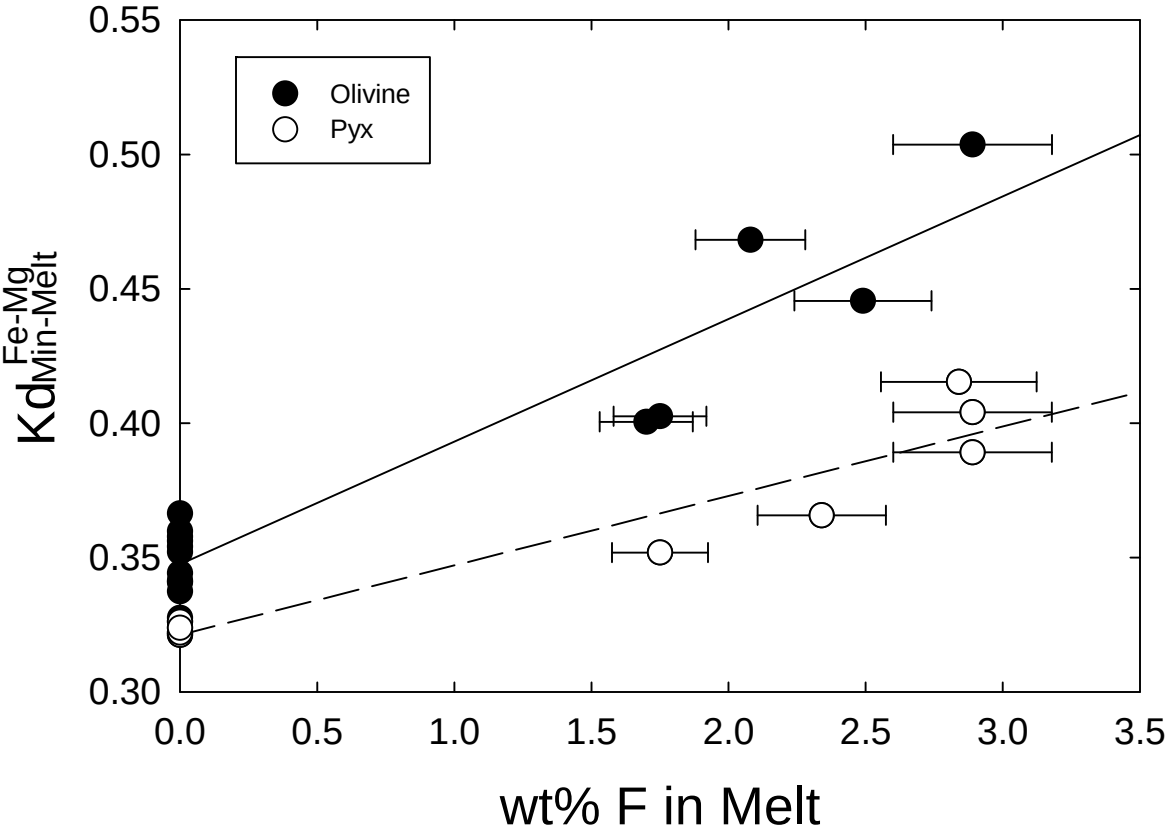
Olivine
Pyx
0.55
0.50
0.45
0.40
0.35
0.30
0.0
0.5
1.0
1.5
2.0
2.5
3.0
3.5
Kd Fe-Mg Min-Melt
wt% F in Melt

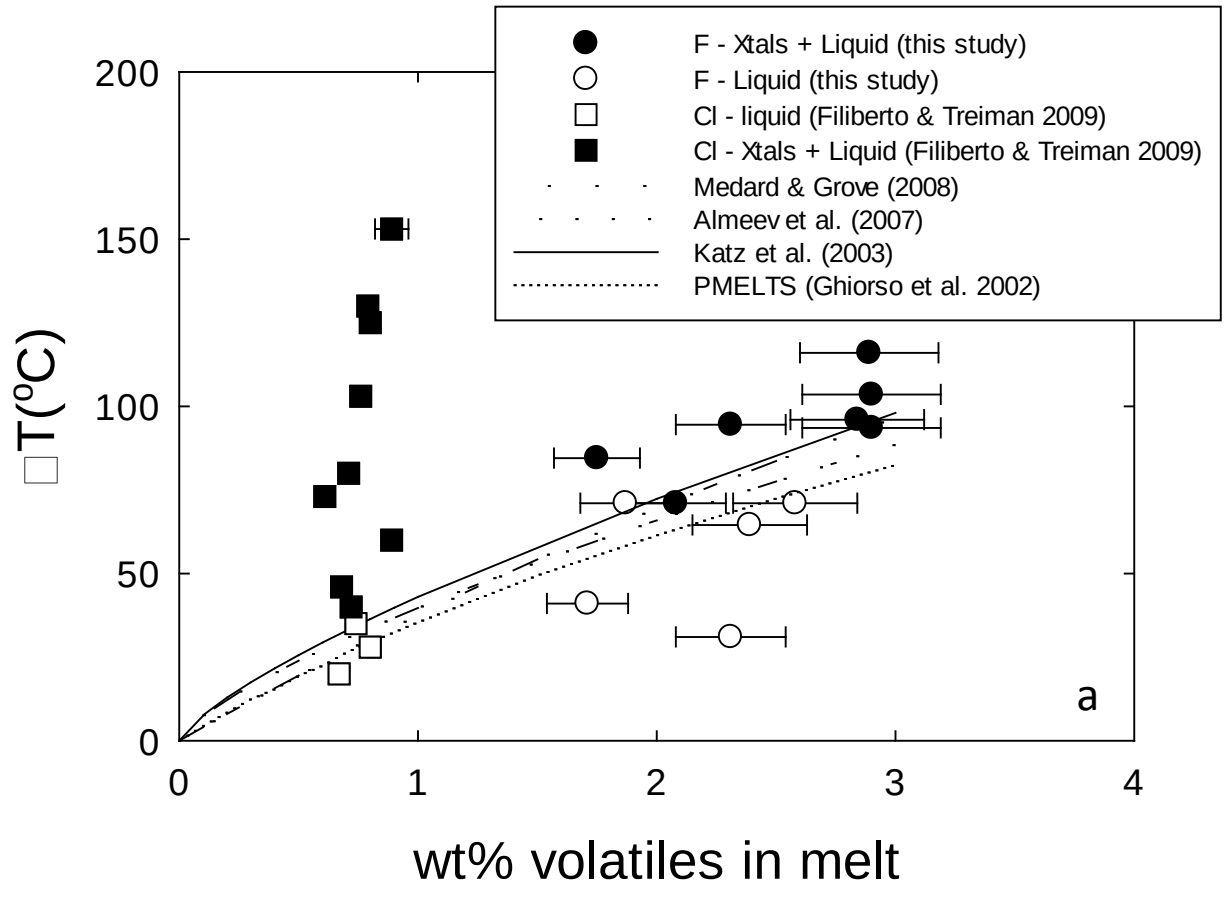
F - Xtals + Liquid (this study)
F - Liquid (this study)
Cl - liquid (Filiberto & Treiman 2009)
Cl - Xtals + Liquid (Filiberto & Treiman 2009)
Medard & Grove (2008)
Almeev et al. (2007)
Katz et al. (2003)
PMELTS (Ghiorso et al. 2002)
□T(°C)
200
150
100
50
0
0
1
2
3
4
a
wt% volatiles in melt

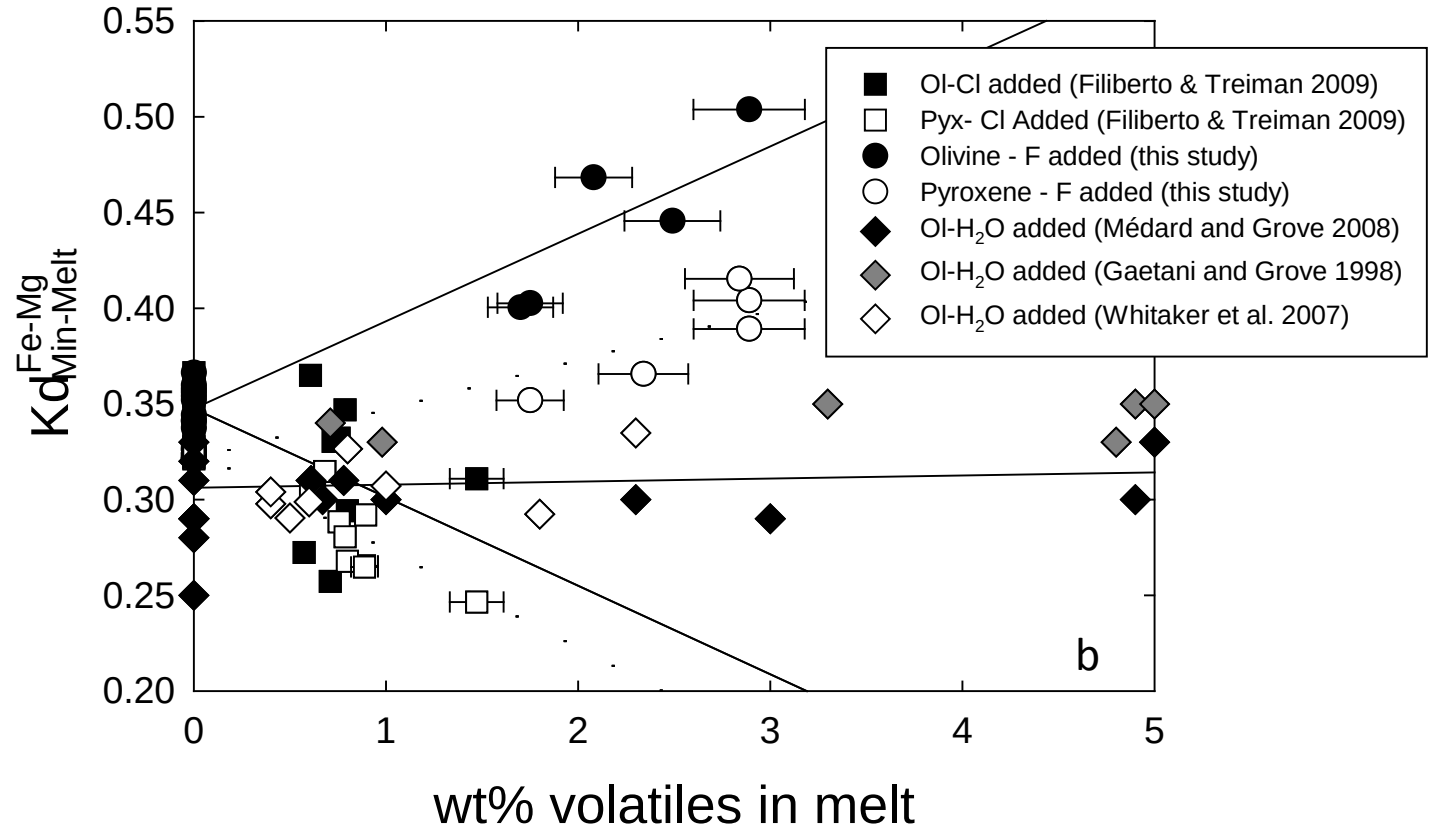
Ol-Cl added (Filiberto & Treiman 2009)
Pyx- Cl Added (Filiberto & Treiman 2009)
Olivine - F added (this study)
Pyroxene - F added (this study)
Ol-H2O added (Médard and Grove 2008)
Ol-H2O added (Gaetani and Grove 1998)
Ol-H2O added (Whitaker et al. 2007)
KdFe-Mg Min-Melt
0.55
0.50
0.45
0.40
0.35
0.30
0.25
0.20
0
1
2
3
4
5
b
wt% volatiles in melt

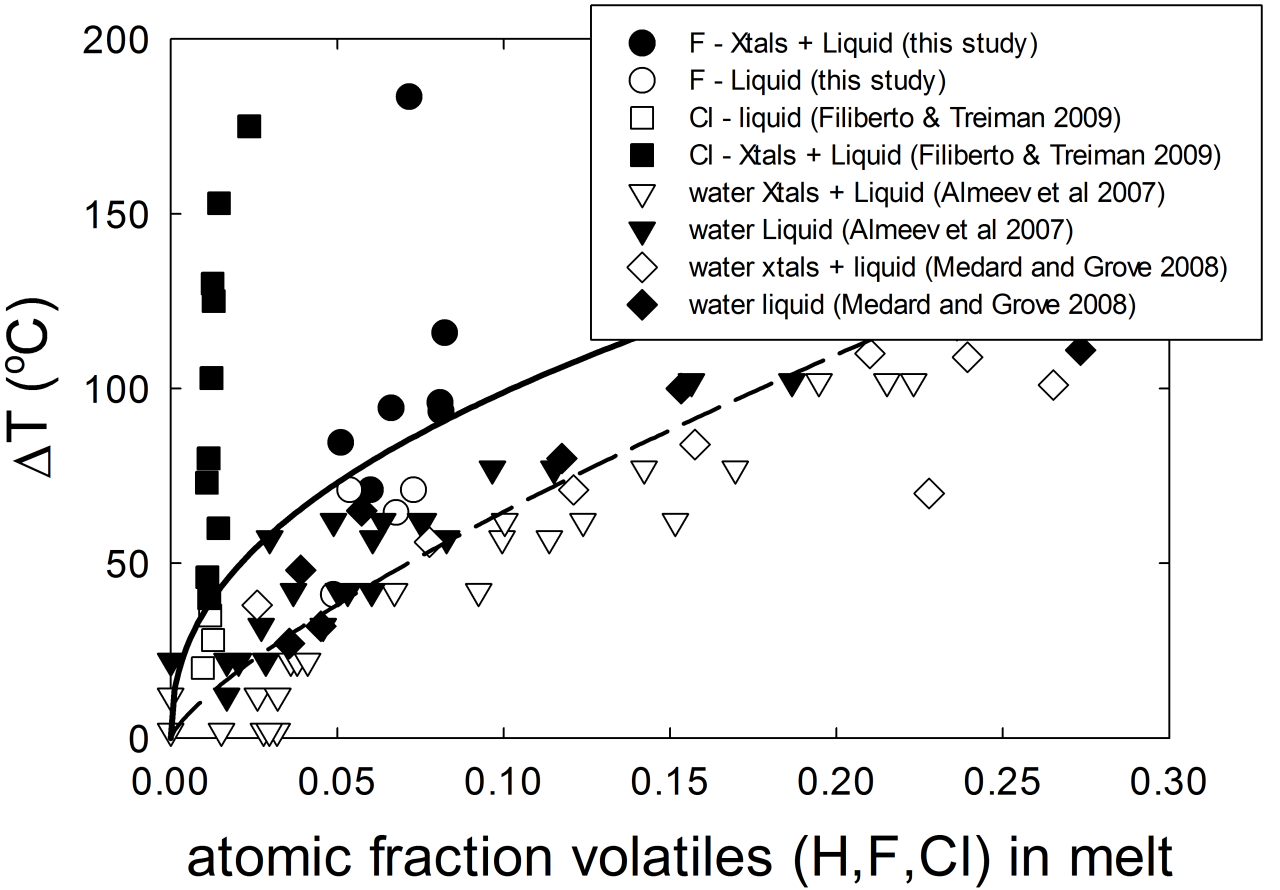
F - Xtals + Liquid (this study)
F - Liquid (this study)
Cl - liquid (Filiberto & Treiman 2009)
Cl - Xtals + Liquid (Filiberto & Treiman 2009)
water Xtals + Liquid (Almeev et al 2007)
water Liquid (Almeev et al 2007)
water xtals + liquid (Medard and Grove 2008)
water liquid (Medard and Grove 2008)
ΔT (°C)
0
50
100
150
200
0.00
0.05
0.10
0.15
0.20
0.25
0.30
atomic fraction volatiles (H,F,Cl) in melt